

Probing the gas that builds planets: Results from the JWST MINDS program

Ewine F. van Dishoeck and the MINDS team

Leiden Observatory, Leiden University, the Netherlands

Abstract. Infrared observations with JWST open up a new window into the chemical composition of the gas in the inner disk (<few au) where planets are built. Results from the MIRI GTO program MINDS are presented for several disks around T Tauri and lower-mass stars. A large diversity in spectra is found. Some disks are very rich in H₂O lines whereas other disks show prominent CO₂. The spectra of disks around very low-mass stars (<0.3 M_⊙, late-M type stars like Trappist-1) are dominated by C₂H₂ and other hydrocarbon features including those of benzene, suggesting volatile C/O>1. Together these data point to a rich chemistry in the inner regions that is linked to the physical structure of these disks (e.g., dust traps) and that may be affected by processes such as radial drift of icy pebbles from the outer to the inner disk.

Keywords. protoplanetary disks, planet formation, molecules, infrared spectroscopy

1. Introduction

Disks around young stars are the birthplaces of planets, but the kind of planets that are formed and their composition varies significantly from star to star and is largely determined by the structure and evolution of their parent disks (Öberg & Bergin 2021). Over the past decade, new observational facilities at millimeter and infrared wavelengths have allowed to study the chemical composition of disks with unprecedented detail. At millimeter wavelengths, the pure rotational transitions of molecules take place, and the Atacama Large Millimeter/submillimeter Array (ALMA) has been key to image a growing number of species (Öberg et al. 2023). Both simple and more complex molecules (Booth et al. 2024) have been probed down to abundances as low as 10⁻¹² with respect to hydrogen and with fully resolved line profiles ($R = \lambda/\Delta\lambda = 10^7$). However, ALMA is limited to the cold outer regions of disks, typically > 10 au.

Infrared observations probe the vibrational transitions of molecules, and, in a few cases (H₂O and OH), also very high-lying pure rotational transitions. The *James Webb Space Telescope* (JWST) provides much higher sensitivity and spectral resolution ($R \approx 3000$) over the 1–28 μm range than previous space missions and uniquely probes the warm inner part of disks (<few au) where terrestrial planets are thought to form. At infrared wavelengths, molecules without a permanent dipole moment can be observed; this includes H₂ as well as carbon-bearing species (e.g., CH₄, C₂H₂, CO₂, ...) down to abundances of ~ 10⁻⁸. Also Polycyclic Aromatic Hydrocarbons (PAHs), ices, silicates and other solid-state species are uniquely probed with infrared data (van Dishoeck 2004). Thus, JWST and ALMA strongly complement each other in studies of the chemistry of planet-forming disks.

The potential of infrared observations for chemical studies of disks became apparent from pioneering ground-based observations (see Brown et al. 2013; Banzatti et al. 2022, 2023b, for recent summaries) as well as initial space-based data from the *Infrared Space Observatory* (e.g., Waelkens et al. 1996) and the *Spitzer Space Telescope* (see Pontoppidan et al. 2014, for review). This brief paper summarizes results obtained with the Mid InfraRed Instrument (MIRI) on JWST (Wright et al. 2023) in the context of the Mid Infrared Disk Survey (MINDS) guaranteed time program (PI: Th. Henning, co-PI: I. Kamp). This 120 hr program observes ~30 disks around solar mass T Tauri stars, ~10 disks around very low-mass stars and brown

dwarfs and a few Herbig and debris disks with the Medium Resolution Spectrometer (MRS) at 5–28 μm (Kamp et al. 2023). Comparison with young disks in the earlier protostellar stages is done in the JWST Observations of Young protoStars (JOYS) MIRI-MRS GTO program (PI: E.F. van Dishoeck, co-PI: H. Beuther) (van Dishoeck et al. 2023; van Gelder et al. 2024). There is also a rapidly growing JWST-MIRI data set on protoplanetary disks based on GO programs, with an additional ~ 150 disks observed in Cycles 1–3 by other teams, most of them part of the JDISCS collaboration (Banzatti et al. 2023a; Pontoppidan et al. 2024).

The goals of the MINDS program are to use JWST to (1) investigate the chemical inventory of the terrestrial planet forming zone, (2) follow the gas evolution into the disk dispersal stage, and (3) study the structure of protoplanetary and debris disks in the thermal mid-IR. The program builds a bridge between the chemical inventory of planet-forming disks and the properties of exoplanets. Here only some highlights related to the first goal will be presented. See Henning et al. (2024) and `minds.cab.inta-csic.es` for an overview and early summary.

2. What sets inner disk abundances?

Three main scenarios affect the inner disk chemistry: (1) high-temperature gas-phase chemistry; (2) drifting icy pebbles from the outer disk followed by sublimation once they cross their snowlines; and (3) dust traps locking up icy pebbles in the outer disk. In addition, time-variable accretion and ejection processes (e.g., winds) play a role in all three cases.

Regarding scenario (1): gas temperatures in the inner disk are high, ranging from 200 K to >1500 K, even exceeding the dust sublimation temperature (Najita et al. 2003; Woitke et al. 2018). UV radiation from the young stars is also enhanced by several orders of magnitude, photodissociating and photoionizing molecules and atoms. Thanks to the high temperatures, reaction barriers can readily be overcome and drive a rapid chemistry that is different from that taking place in the cold outer part (Walsh et al. 2015). One important case is the balance between H_2O and CO_2 through the intermediate OH: at 100–250 K, OH reacts primarily with CO to form CO_2 , but at higher temperatures it reacts with H_2 to form H_2O (van Dishoeck et al. 2023). Because of continuum optical depth at mid-IR wavelengths, JWST observations are limited to the upper layers of the disk (e.g., Bruderer et al. 2015), although grain growth and settling to the midplane make it possible to look deeper into the disk. Indeed, effective gas/(small) dust ratios in the infrared emitting layers are typically 10000 rather than 100 (Meijerink et al. 2009).

The C/O ratio is thought to be an important diagnostic for linking exoplanets with their formation location (Öberg et al. 2011). In the inner disk, dust temperatures are high enough that all ices have sublimated so the C/O ratio in the gas should be close to the stellar value: the chemistry reshuffles the individual molecular abundances but does not affect the overall C/O.

Scenarios (2) and (3) alter the C/O (and C/H and O/H) abundances ratios in the inner region (see Figure 1). In scenario (2), water (and more generally oxygen, O/H) is enhanced by the drifting of water-rich icy pebbles from the outer to the inner disk. Once icy grains cross the disk mid-plane snowline around ~ 160 K, the water ice sublimates into the gas and becomes visible to JWST if mixed to high enough altitudes. Enhancements in O/H can be more than an order of magnitude compared to the interstellar value (e.g., Bosman et al. 2018; Kalyaan et al. 2021; Mah et al. 2023). Indeed, several JWST spectra show evidence for enhanced “cold” (~ 200 K) water at the water snowline (Banzatti et al. 2023a, 2024; Temmink et al. 2024a). This enhancement is expected to be particularly strong for disks that show compact dust millimeter continuum emission with ALMA and large ratios of their gas/dust radii, indicative of pebbles that have drifted inwards (Banzatti et al. 2020; Trapman et al. 2019). Similarly, CO and carbon-containing icy grains can drift in and enhance C/H (e.g., Zhang et al. 2020).

The opposite case holds for disks with gaps and cavities that show prominent dust rings (“substructures”) with ALMA (Andrews 2020). In scenario (3), these rings can trap the icy dust grains and prevent them from moving inwards, thereby lowering the inner disk O/H and

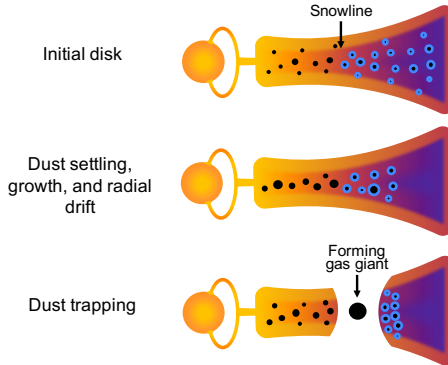


Figure 1. Cartoon illustrating the three scenarios of a full initial disk (top), a disk with significant grain growth, settling and radial drift of icy pebbles (middle) and a disk with a gap, locking up icy pebbles in a dust trap. Figure by Sierra Grant.

C/H ratios significantly. Much depends on the timing of the formation of these dust traps (Mah et al. 2024; Sellek et al. 2024): if they form early (< 1 Myr), the initial inner disk water rapidly drains onto the star and the disk becomes very dry.

By comparing inner disk abundances found with JWST with disk structures imaged by ALMA, scenarios (2) and (3) can be tested. One caveat is that ALMA can only image cavities at best down to a few au for nearby disks. This is also the region where the millimeter continuum becomes optically thick making it more difficult to see small gaps. The structure of disks inside a few au is therefore still largely unknown territory, although near-IR interferometry and spectrally resolved CO data are providing some constraints.

3. Results

3.1. *T Tauri disks*

Figure 2 summarizes the 13–17 μm spectrum of three disks around T Tauri stars: GW Lup, DR Tau and DF Tau (Grant et al. 2023, 2024; Temmink et al. 2024a,b). The bottom part shows the simulated spectra of the various molecules that contribute to the emission in this region. These so-called slab models assume that the level populations of each molecule are in LTE at a single temperature T with the column density N and emitting area Ω determining the strength of the lines. Typical temperatures are 600–800 K for C_2H_2 and HCN and 300–400 K for CO_2 , with emission coming from the inner ~ 0.3 au. H_2O has many lines throughout the MIRI wavelength range indicating a temperature gradient roughly as $R^{-0.5}$ from ~ 1200 K down to ~ 180 K over the 0.1 – few au range (Gasman et al. 2023; Temmink et al. 2024a), as also found in JDISCS (Romero-Mirza et al. 2024).

It is clear that there is significant diversity among disks: many T Tauri disks are bright in H_2O lines (e.g., DR Tau, DF Tau) whereas others show particularly strong CO_2 features (e.g., GW Lup), including $^{13}\text{CO}_2$ (Grant et al. 2023) and even CO^{18}O (e.g., CX Tau, Vlasblom et al. subm.). The detection of isotopologs indicates that the main $^{12}\text{CO}_2$ band is optically thick and that the $\text{CO}_2/\text{H}_2\text{O}$ column density ratio is much higher than would be suggested by the relative strengths of the lines. The CO_2 isotopologs are also fitted with colder temperatures suggesting that they are located deeper in the disk (Bosman et al. 2022).

What causes this diversity? DR Tau has a compact millimeter dust disk, whereas DF Tau is a 9 au separation binary system with very small truncated dust disks around both components. Thus, radial drift of icy grains followed by water sublimation in the inner disk could play a

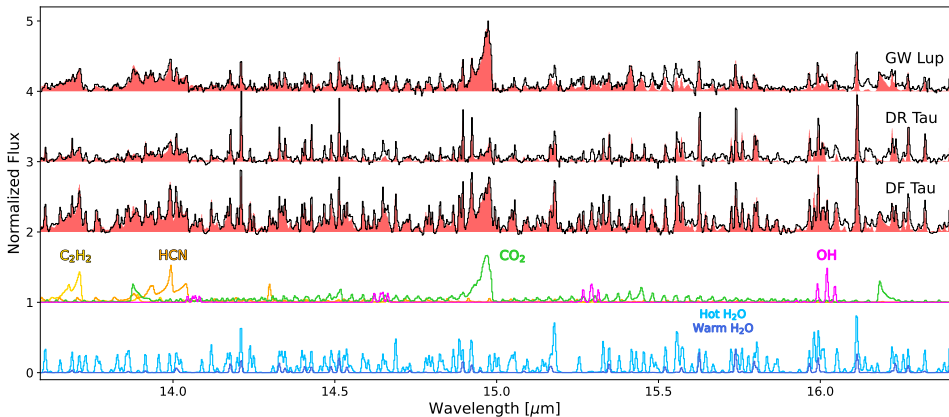


Figure 2. Continuum-subtracted MIRI spectra (black) compared to a best-fitting total model in red, for the disks around GW Lup, a large dust disk with rings (top); DR Tau, a compact dust disk (second row); and DF Tau, a close binary (third row). The spectra are normalized to the peak emission in this wavelength range, 0.035 Jy for GW Lup, 0.52 Jy for DR Tau, and 0.27 Jy for DF Tau (note the much weaker lines of GW Lup). Model emission from C_2H_2 (yellow), HCN (orange), CO_2 (green) and OH (pink) is presented in the fourth row for parameters that best fit the DF Tau disk emission. The bottom row shows two H_2O models in cyan (920 K) and blue (490 K). Data and models taken from [Grant et al. \(2023\)](#); [Temmink et al. \(2024b,a\)](#); [Grant et al. \(2024\)](#), see those papers for best fitting values. Figure by Sierra Grant.

role for these disks (§ 2). In contrast, GW Lup has a large dust disk with dust rings that can trap the icy pebbles at large radii well beyond the snowlines.

However, not all compact dust disks are bright in water lines. CX Tau is an example of a drift-dominated disk with brighter CO_2 than H_2O lines (Vlasblom et al., *subm.*). Thermochemical models suggest a number of factors that can enhance one species over the other (Vlasblom et al. 2024). For example, a small cavity between the H_2O and CO_2 snowlines can selectively remove H_2O . Also, temperature plays a role (§ 2): at low T , OH will react with CO to form CO_2 rather than with H_2 to form H_2O . Finally, the age of the disk can affect relative abundances (Sellek et al. 2024): CO_2 -rich ices drift in later than H_2O -rich ices.

Another sign that the situation may be more complex than sketched in § 2 is the detection of water in the inner region of the transitional disks. PDS 70 is a well-known disk with a large cavity in which two young giant planets have been detected (Keppler et al. 2018; Haffert et al. 2019). The prominent dust ring at 45 au is thought to trap all the drifting icy pebbles and prevent them from entering the small (few au) inner disk. It therefore came as a surprise when JWST clearly detected water at $T \approx 600$ K from the inner disk (Perotti et al. 2023). Similarly, emission of water and other molecules is detected from the inner region of the transitional disk SY Cha with a large 70 au cavity (Schwarz et al. 2024). A systematic study of several gapped T Tauri disks in the MINDS sample reveals emission of water and other species from the inner disk in all cases (Gasman et al., *subm.*). This suggests that gaps do not fully block the delivery of oxygen- and carbon-containing gas and (small, icy) dust to the inner disk: dust traps are clearly “leaky” even if the dust and gas cavities are broad and deep.

Taken together, the data indicate that the gas in the inner disks of T Tauri stars is generally oxygen rich, with $C/O < 1$: H_2O is usually the most abundant molecule, followed closely by CO_2 . C_2H_2 and HCN typically have about two orders of magnitude lower column densities. CH_4 is generally not detected (Temmink, *priv. comm.*). OH is never a significant reservoir of oxygen, although it is a unique probe of the UV field and high-temperature chemistry (Tabone et al. 2024). Note that the various molecules are not necessarily co-located, neither radially nor vertically in the disk, so any column density ratios should be interpreted with caution. More

generally, inner disk chemistry may be less strongly related to outer disk substructures than previously thought.

3.2. Disks around very low-mass stars and brown dwarfs

The JWST spectra of disks around very low mass stars (VLMS, $<0.3 M_{\odot}$) and brown dwarfs ($<0.08 M_{\odot}$) are generally very different from those around T Tauri stars. VLMS are of particular interest since late M-type stars (later than M4) are the most common stars in the Galaxy, and many rocky exoplanet studies focus on them, with the Trappist-1 system being the most famous example. Early hints for bright C_2H_2 emission from VLMS disks came from *Spitzer* spectra (Pascucci et al. 2013), but JWST reveals their rich hydrocarbon emission in unprecedented detail.

The first JWST example was the J16053215-1933159 (J1605) disk which shows two prominent broad bumps at 7.7 and 13.7 μm (Tabone et al. 2023). These can be ascribed to highly optically thick C_2H_2 emission in its $\nu_4+\nu_5$ and ν_5 bands, with orders of magnitude higher column densities ($> 10^{20} \text{ cm}^{-2}$) at 525 K coming from the inner 0.033 au. Larger hydrocarbons such as C_4H_2 and C_6H_6 (benzene) are also prominent and detected for the first time.

Subsequent JWST studies have revealed other VLMS disk examples with very rich hydrocarbon spectra, although not with such prominent C_2H_2 bumps as J1605. Rather, the many *P*- and *R*-branch lines of hydrocarbon molecules like CH_4 and C_2H_4 form an underlying pseudo-continuum on which their *Q*-branches are detected (Arabhavi et al. 2024; Kanwar et al. 2024a). C_2H_6 is also detected in a disk for the first time. Of the oxygen-bearing species, CO_2 is detected, but CO only sporadically and H_2O is weak, if detected at all (Tabone et al. 2023; Arabhavi et al. 2024). There appear to be a few exceptions: the disk around the VLMS Sz 114 ($0.17 M_{\odot}$) shows prominent H_2O lines resembling more that of T Tauri stars (Xie et al. 2023).

Chemical modeling shows that such high abundances of hydrocarbon molecules can only be achieved if $C/O > 1$ in the emitting layers (Kanwar et al. 2024b). This means that either carbon is enhanced, or oxygen is depleted, or both. Mechanisms for enhancing carbon include the destruction of hydrocarbon grains at ~ 500 K (a so-called “soot” line, Li et al. 2021) or the drifting in of hydrocarbon-rich ices that are subsequently eroded (Tabone et al. 2023; Mah et al. 2024). Options for oxygen depletion focus on locking up most of the oxygen in H_2O ice in a dust trap outside the water snowline. Quantification of these models requires better constraints on the actual H_2O emission which is hidden below the forest of hydrocarbon lines in VLMS disks (Arabhavi et al., *subm.*). If C/O is indeed > 1 , this may have consequences for the chemical composition of (terrestrial) planets that are forming in the inner disk. As for Earth, the planets may be poor in carbon if most of the solid carbon has been removed from the disk in the form of carbon-rich gas.

4. Conclusions

The first two years of JWST data have revealed a large diversity in the spectra of protoplanetary disks. It is clear that stellar mass, the presence of dust traps in the inner and/or outer disk, radial drift of icy pebbles, and the age and history of the system all play a role in setting inner disk abundances where planets are formed. Much larger samples are needed to reveal systematic trends, if any, and linking them to exoplanet composition statistics. The community can look forward to many more JWST disk spectra in the coming years.

Acknowledgments. The author is grateful to the entire MINDS team and the MIRI consortium for many years of fruitful collaborations. Special thanks to Sierra Grant for providing Figures 1 and 2. This work is supported by A-ERC grant 101019751 MOLDISK.

References

- Andrews, S. M. 2020, *ARAA*, 58, 483
- Arabhavi, A. M., Kamp, I., Henning, T., et al. 2024, *Science*, 384, 1086
- Banzatti, A., Abernathy, K. M., Brittain, S., et al. 2022, *AJ*, 163, 174
- Banzatti, A., Pascucci, I., Bosman, A. D., et al. 2020, *ApJ*, 903, 124
- Banzatti, A., Pontoppidan, K. M., Carr, J. S., et al. 2023a, *ApJ*, 957, L22
- Banzatti, A., Pontoppidan, K. M., P ere Ch avez, J., et al. 2023b, *AJ*, 165, 72
- Banzatti, A., Salyk, C., Pontoppidan, K. M., et al. 2024, arXiv e-prints, arXiv:2409.16255
- Booth, A. S., Temmink, M., van Dishoeck, E. F., et al. 2024, *AJ*, 167, 165
- Bosman, A. D., Bergin, E. A., Calahan, J. K., & Duval, S. E. 2022, *ApJ*, 933, L40
- Bosman, A. D., Walsh, C., & van Dishoeck, E. F. 2018, *A&A*, 618, A182
- Brown, J. M., Pontoppidan, K. M., van Dishoeck, E. F., et al. 2013, *ApJ*, 770, 94
- Bruderer, S., Harsono, D., & van Dishoeck, E. F. 2015, *A&A*, 575, A94
- Gasman, D., van Dishoeck, E. F., Grant, S. L., et al. 2023, *A&A*, 679, A117
- Grant, S. L., Kurtovic, N. T., van Dishoeck, E. F., et al. 2024, *A&A*, 689, A85
- Grant, S. L., van Dishoeck, E. F., Tabone, B., et al. 2023, *ApJ*, 947, L6
- Haffert, S. Y., Bohn, A. J., de Boer, J., et al. 2019, *Nature Astronomy*, 3, 749
- Henning, T., Kamp, I., Samland, M., et al. 2024, *PASP*, 136, 054302
- Kalyaan, A., Pinilla, P., Krijt, S., Mulders, G. D., & Banzatti, A. 2021, *ApJ*, 921, 84
- Kamp, I., Henning, T., Arabhavi, A. M., et al. 2023, *Faraday Discussions*, 245, 112
- Kanwar, J., Kamp, I., Jang, H., et al. 2024a, *A&A*, 689, A231
- Kanwar, J., Kamp, I., Woitke, P., et al. 2024b, *A&A*, 681, A22
- Kepler, M., Benisty, M., M uller, A., et al. 2018, *A&A*, 617, A44
- Li, J., Bergin, E. A., Blake, G. A., Ciesla, F. J., & Hirschmann, M. M. 2021, *Science Advances*, 7, eabd3632
- Mah, J., Bitsch, B., Pascucci, I., & Henning, T. 2023, *A&A*, 677, L7
- Mah, J., Savvidou, S., & Bitsch, B. 2024, *A&A*, 686, L17
- Meijerink, R., Pontoppidan, K. M., Blake, G. A., Poelman, D. R., & Dullemond, C. P. 2009, *ApJ*, 704, 1471
- Najita, J., Carr, J. S., & Mathieu, R. D. 2003, *ApJ*, 589, 931
-  berg, K. I. & Bergin, E. A. 2021, *Phys. Rep.*, 893, 1
-  berg, K. I., Boogert, A. C. A., Pontoppidan, K. M., et al. 2011, *ApJ*, 740, 109
-  berg, K. I., Facchini, S., & Anderson, D. E. 2023, *ARAA*, 61, 287
- Pascucci, I., Herczeg, G., Carr, J. S., & Bruderer, S. 2013, *ApJ*, 779, 178
- Perotti, G., Christiaens, V., Henning, T., et al. 2023, *Nature*, 620, 516
- Pontoppidan, K. M., Salyk, C., Banzatti, A., et al. 2024, *ApJ*, 963, 158
- Pontoppidan, K. M., Salyk, C., Bergin, E. A., et al. 2014, *Protostars & Planets VI*, ed. Beuther, H., Klessen, R., Dullemond, K., Henning, Th. (Tucson: Univ. Arizona Press), 363–385
- Romero-Mirza, C. E., Banzatti, A.,  berg, K. I., et al. 2024, *ApJ*, 975, 78
- Schwarz, K. R., Henning, T., Christiaens, V., et al. 2024, *ApJ*, 962, 8
- Sellek, A. D., Vlasblom, M., & van Dishoeck, E. F. 2024, arXiv e-prints, arXiv:2412.01895
- Tabone, B., Bettoni, G., van Dishoeck, E. F., et al. 2023, *Nature Astronomy*, 7, 805
- Tabone, B., van Dishoeck, E. F., & Black, J. H. 2024, *A&A*, 691, A11
- Temmink, M., van Dishoeck, E. F., Gasman, D., et al. 2024a, *A&A*, 689, A330
- Temmink, M., van Dishoeck, E. F., Grant, S. L., et al. 2024b, *A&A*, 686, A117
- Trapman, L., Facchini, S., Hogerheijde, M. R., van Dishoeck, E. F., & Bruderer, S. 2019, *A&A*, 629, A79
- van Dishoeck, E. F. 2004, *ARAA*, 42, 119
- van Dishoeck, E. F., Grant, S., Tabone, B., et al. 2023, *Faraday Discussions*, 245, 52
- van Gelder, M. L., Francis, L., van Dishoeck, E. F., et al. 2024, arXiv e-prints, arXiv:2410.01636
- Vlasblom, M., van Dishoeck, E. F., Tabone, B., & Bruderer, S. 2024, *A&A*, 682, A91
- Waelkens, C., Waters, L. B. F. M., de Graauw, M. S., et al. 1996, *A&A*, 315, L245
- Walsh, C., Nomura, H., & van Dishoeck, E. 2015, *A&A*, 582, A88
- Woitke, P., Min, M., Thi, W. F., et al. 2018, *A&A*, 618, A57
- Wright, G. S., Rieke, G. H., Glasse, A., et al. 2023, *PASP*, 135, 048003
- Xie, C., Pascucci, I., Long, F., et al. 2023, *ApJ*, 959, L25
- Zhang, K., Bosman, A. D., & Bergin, E. A. 2020, *ApJ*, 891, L16